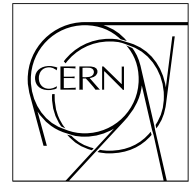


The Compact Muon Solenoid Experiment

# CMS Note

Mailing address: CMS CERN, CH-1211 GENEVA 23, Switzerland



November 6, 2007

## CMS DT Chambers: Correction of drift non-linearity

P. Bortignon, S. Pesente, S. Vanini, G. Zumerle

*University of Padova and INFN Padova, Italy*

### Abstract

The non-linearity in the space-drift time relation of the DT drift cell, as a function of the track angle, has been measured using cosmic ray data. The improvement obtained in the track reconstruction precision is presented.

*t bias, version 0*

# 1 Introduction

The DT drift cell design has been optimized to obtain a linear relation between drift space and time. This was in fact an essential requirement to allow the use of the DT chambers as a first level trigger device, through the mean-timing technique (riferimento). The residual non-linearity effects, more important for large angle tracks, can be corrected during the off line track reconstruction. A method is presented to compute the non-linearity of the space-time relation as a function of the track impact point and angle. The parametrization of the drift time non linearity is then used to obtain a more accurate measurement of the track coordinates. The results obtained with this technique, and the improvement in reconstruction precision obtained, are presented.

The analysis presented in this Note is based on a sample of (quanti, un milione?) cosmic ray tracks collected with two MB3 spare DT chambers, MB3-061 and MB3-054, presently located in the INFN "Laboratori Nazionali di Legnaro". The chambers were operated in autotrigger mode.

Figure 1 shows the track coordinate and angle measured by the Phi Superlayers for the data sample used in the analysis of the present note.

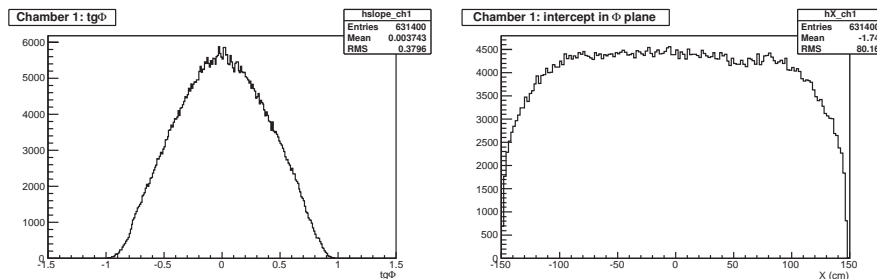


Figure 1: Track impact point and track angle measured by the chamber Phi Superlayers for the cosmic ray track sample used in the analysis presented in the note.

# 2 The DT Chambers drift cell

The cross section of the drift tube of the CMS DT chambers is shown schematically in Figure 2. The dimension of the cell is  $42 \times 13 \text{ mm}^2$ . The electric field in the drift cell is shaped by three electrodes: a wire, kept at positive voltage, where the electron multiplication occurs, two cathodes at negative voltage, and two central strip electrodes with voltage intermediate between wire and ground, whose purpose is to improve the field uniformity along the drift path.

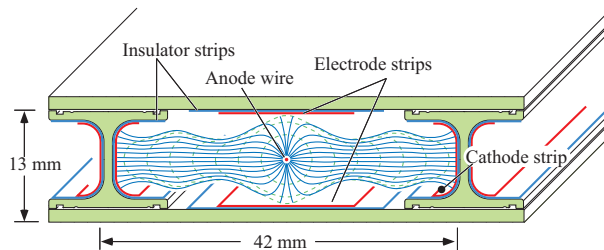


Figure 2: Schematic view of a drift tube. The drift lines (continuous lines) and the isochronous surfaces (dotted lines), computed with the CERN program GARFIELD [5], are also shown.

The cell electrostatic configuration has been designed to have an almost constant drift velocity along the full drift path. This was in fact an essential requirement to use the chamber output in the CMS first level trigger using the so called Mean Timer algoritm (riferimento). For the algorithm to work, the ionization electrons drift time must be proportional to the distance from the wire of the track intersection with the wire plane. The linearity assumption has been measured to be quite accurate using high energy test beams (reference), at least for tracks almost perpendicular to the chamber plane. However, when the track projection in a plane normal to the wires presents a large angle with respect to the perpendicular to the wire plane, two effects becomes important, as can be seen in Figure 3:

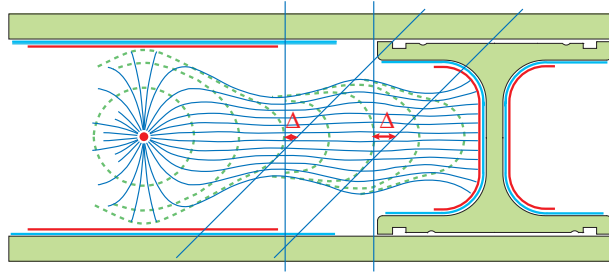


Figure 3: Sketch of the origin of non-linearity for inclined tracks.

1. The drift time is measured using the leading edge of the wire signal, that is created by the electrons arriving first to the wire. Those electrons start from the middle plane of the chamber only for perpendicular tracks.
2. For inclined tracks, the difference in arrival time between the first electrons and the electrons starting from the middle plane depend not only from the track angle, but also from the track distance from the wire.

The average correction of the first effect has been discussed and measured in [2]. On average over the full drift length the drift time has been measured to be shorter than expected by the quantity  $\Delta t = -K \cdot (tg\Phi)^2$ , with  $K = (19.79 \pm 0.04) \text{ ns}$ .

The existence of a sizeable residual non-linearity is evident from the so called Time box distribution, i.e. the histogram of the drift times measured with a uniform illumination of the drift cells. Neglecting the effects arising from the time measurement resolution, we can write (non so scrivere le formule)  $\Delta N/\Delta t = (\Delta N/\Delta x) \cdot (\Delta x/\Delta t) = k \cdot v_{drift}$ . In presence of a uniform illumination  $k$  is a constant, and the time box histogram shape reflects directly how the drift velocity changes as a function of the distance from the wire position.

In Figure 4 two examples of "time-box" histograms are shown, for two angular intervals of the track direction. The non linearity of the time-space relation, and its dependance on the track angle are quite evident.

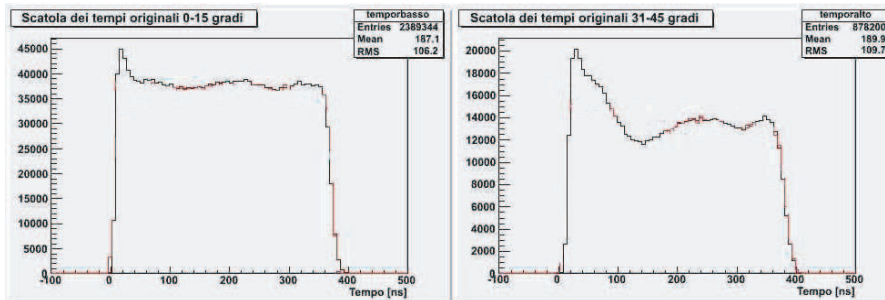


Figure 4: Example of cosmic ray raw time histograms.

The parametrization of the drift time non linearity has been addressed in reference [4], using the simulation of the drift cell given by the program GARFIELD, also in presence of a magnetic field. Their results in absence of magnetic field are shown in Figure 5

In this note we want to measure the drift time non linearity as a function of the track position and angle using real cosmic ray tracks. The parametrization of the non linearity is then used to improve the track reconstruction accuracy.

### 3 The method

We use the track measurements in the Phi plane, selecting events for which a successful 8 points track fit has been obtained, using the fit method discussed in [2]. For the tracks of this sample, we repeat the fit discarding one of the 8 points, and compute the distance  $\Delta x$  between the wire whose signal has been discarded and the fitted track intersection with the wire plane. Since the two track parameters are constrained by seven points with a long lever arm, we assume that the systematic error on the intersection point is much smaller than the non linearity effect on a single drift time measurement. We then compute the expected drift time in a linear approximation as

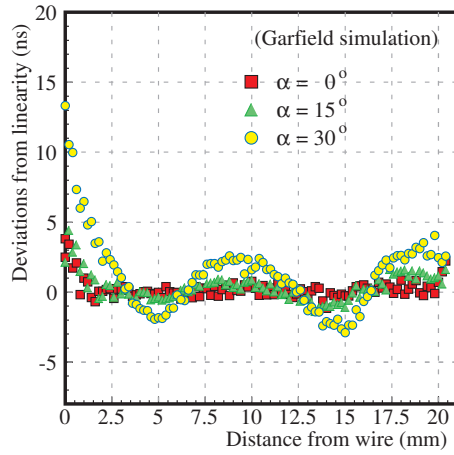


Figure 5: Deviations from linearity computed using the GARFIELD program. Figure taken from reference [4]

$t_{lin} = \Delta x / v_{drift}$ , using for  $v_{drift}$  the value of  $v_D = 54.7 \mu\text{m}/\text{ns}$  measured with the method described in [2], and the difference with the actual drift time measurement,  $t_{meas}$ , equal to  $\Delta t = t_{meas} - t_{lin}$ . The procedure is repeated for all the 8 points of the track, and for all the tracks. The  $\Delta t$  quantities for tracks of a given angular interval, and for small bins of  $\Delta x$  are finally histogrammed. Figure 6 shows a sample of such histograms. The mean value of the histograms, is computed fitting a gaussian function, discarding the tails outside  $2.5\sigma$ .

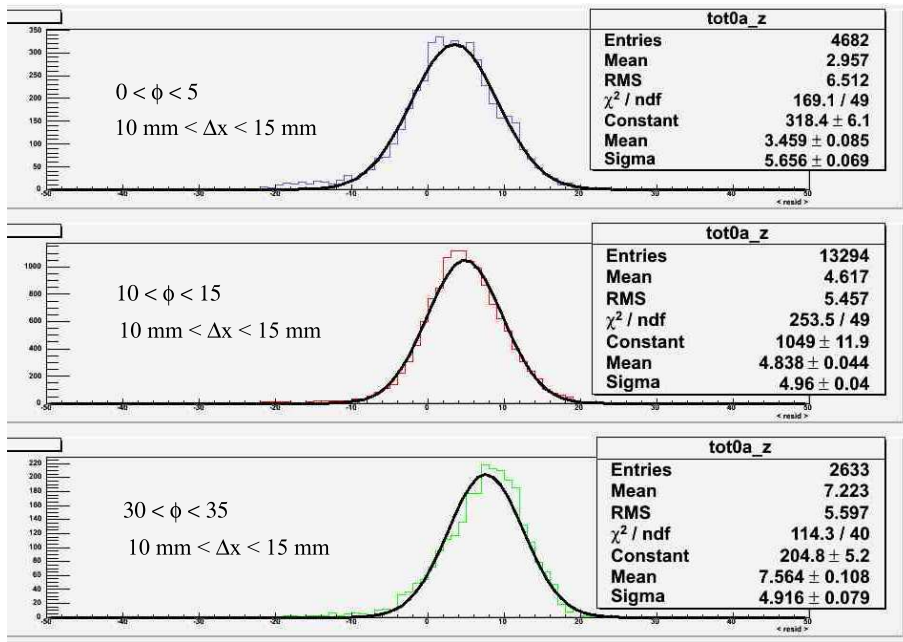


Figure 6: Histograms of deviations from linearity. See text for the method to compute them

If the drift space - time relation was linear, the gaussian centre would be zero within the measurement error. We can see from Figure 6 that this is not true. The mean value is significantly different from zero, and changes with the angle of the track. We take  $\langle \Delta t \rangle$  as the measurement of the non linearity. Plotting  $\langle \Delta t \rangle$  as a function of the wire distance  $\Delta x$  for tracks of a given angular interval we can cross check the results of reference [4]. Figure 7 shows a sample of such plots.

The experimental results of Figure 7 can be compared with the simulation results shown in Figure 5. Although not identical, the main features of the two set of plots are quite similar.

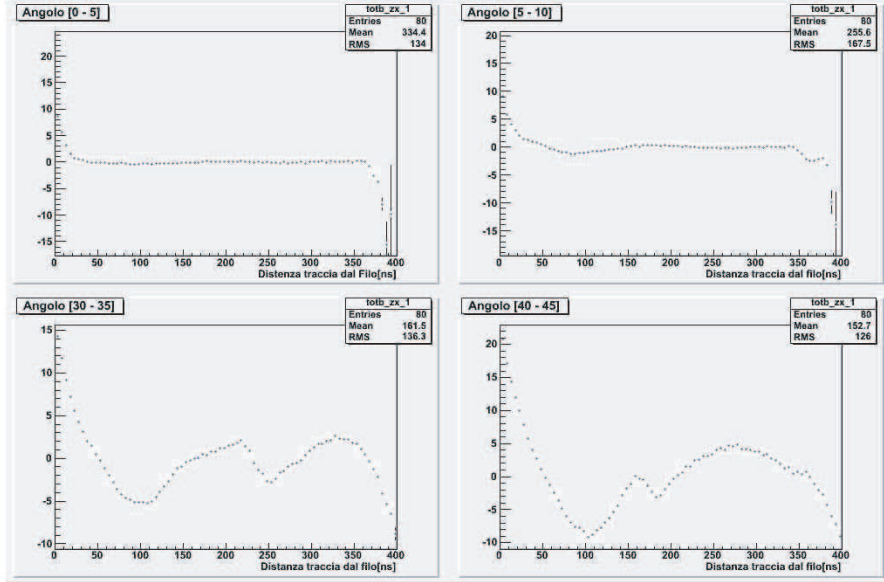


Figure 7: Deviations from linearity for four angles, as a function of the track distance from the wire in the wire plane.

## 4 Correction of experimental data

Our purpose is to correct the measured drift times to restore the linearity between drift space and time. The plots shown in Figure 7 are not directly usable for this purpose, because they give the correction as a function of the true track position, while we start from the “distorted” drift time. We can however follow the procedure explained in the previous section, but plot the  $\langle \Delta t \rangle$  quantity as a function of the measured drift time. The scatter plot of  $\Delta t$  versus the measured drift time  $t_{meas}$  is plotted in Figure 8 for two values of the track incidence angle.

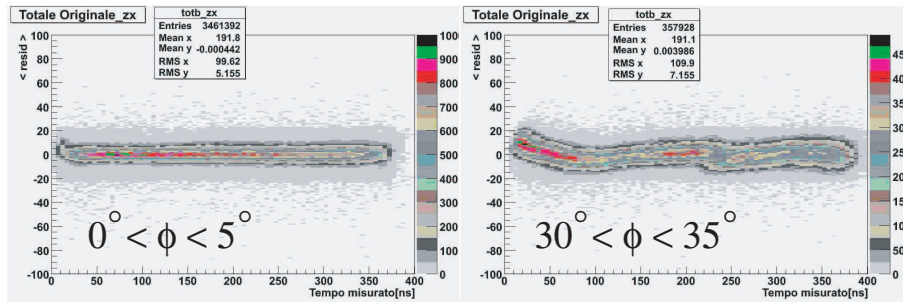


Figure 8: Deviations from linearity for four angles, as a function of the track distance from the wire in the wire plane.

Again the non-linearity is evident, as well its dependence from the track angle.

Averaging the  $\Delta t$  residuals in small  $t_{meas}$  bins produces the plots of Figure 9.

As a first cross check of the procedure we have repeated the full process starting from the corrected drift times. In an ideal situation, all the  $\langle \Delta t \rangle$  values should now come out compatible with zero.

Figure 10 shows the resulting plots. The second order corrections are not zero, but are anyway much smaller than the first order ones, being always smaller than  $\sim 2ns$ , corresponding to less than  $100\mu m$  of drift space. For this reason we decided to stop the procedure after the first iteration.

## 5 Results

We do not have an independent precise detector to certify that after the non-linearity correction the track reconstruction accuracy has improved. In addition, cosmic rays have an important component with very low momentum, and

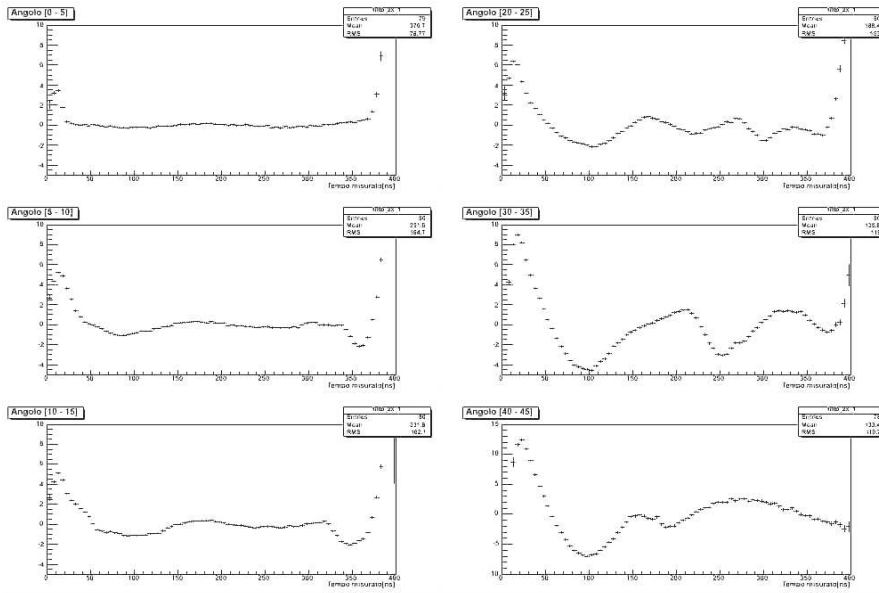


Figure 9: Deviations from linearity as a function of the measured drift time, for several track angle intervals.

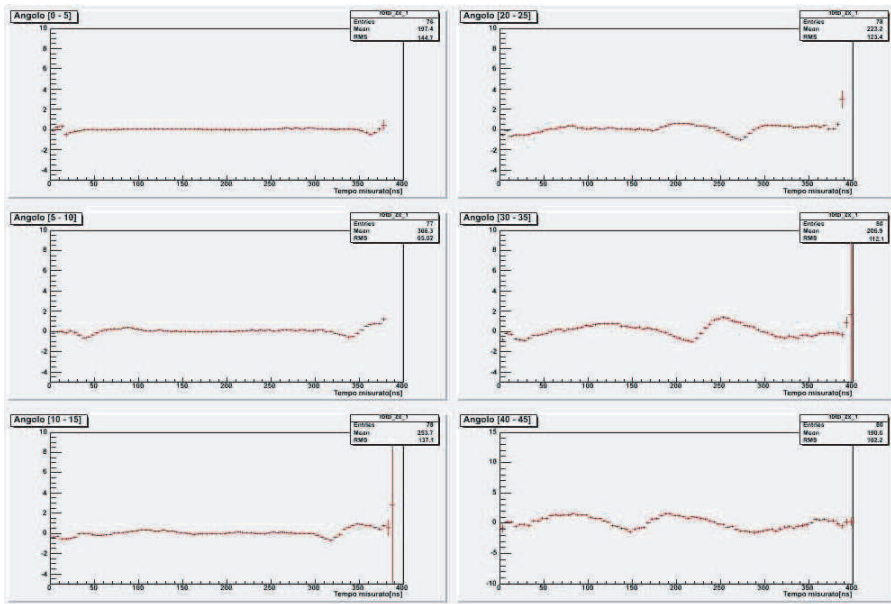


Figure 10: Deviations from linearity as a function of the measured drift time, for several track angle intervals, starting from drift times corrected for the non linearity.

the multiple scattering would make the comparison not straightforward. What we can do is to show that residuals of the track fit after the corrections are significantly better. This can be seen in Figure 11, where the sum of the fit residuals squared is shown before and after the correction, and in Figure 12, where the fit residual rms is shown as a function of the track angle. We see that the improvement is more important for large angle tracks, as expected.

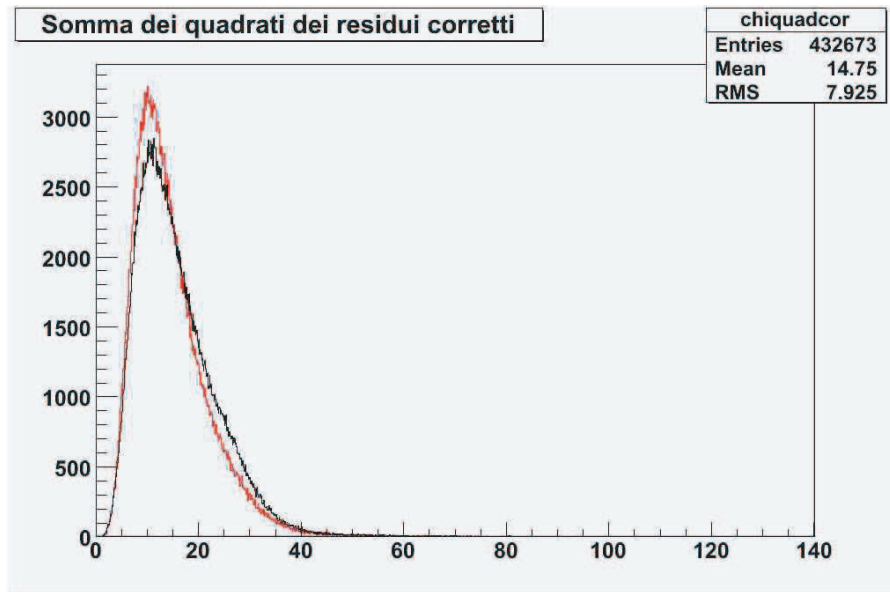


Figure 11: Sum of the fit residuals squared before and after the drift time correction.

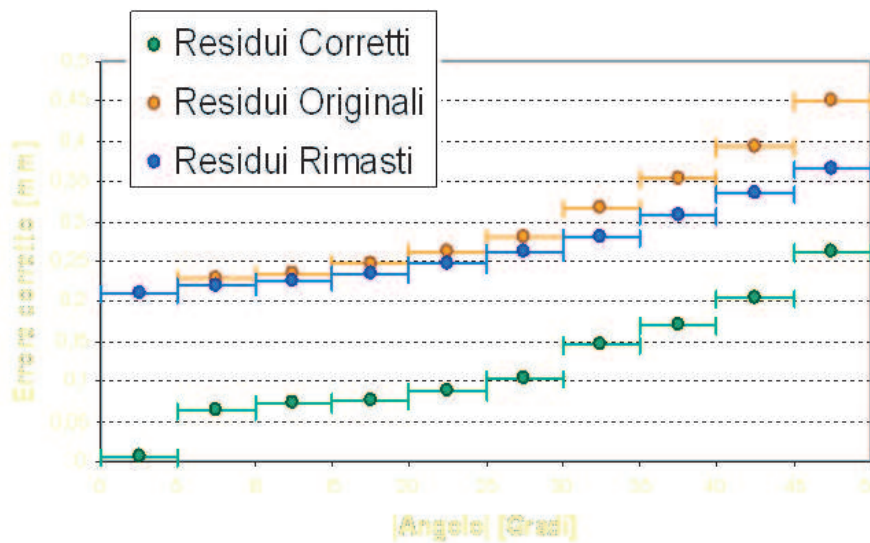


Figure 12: Residual rms as a function of the track angle, before and after the drift time correction.

As last check, we show in Figure 13 the timebox histograms, before and after correction, for several track angle intervals. After correction, the histograms are practically flat, with the exception of a small region of small drift times.

## 6 Conclusions

We have presented a method to experimentally measure the exact dependence of the drift time in the CMS DT chambers on the track crossing point and angle. The method has been applied using a sample cosmic ray tracks in absence of magnetic field, showing that non linearity effects are negligible for track perpendicular to the chamber

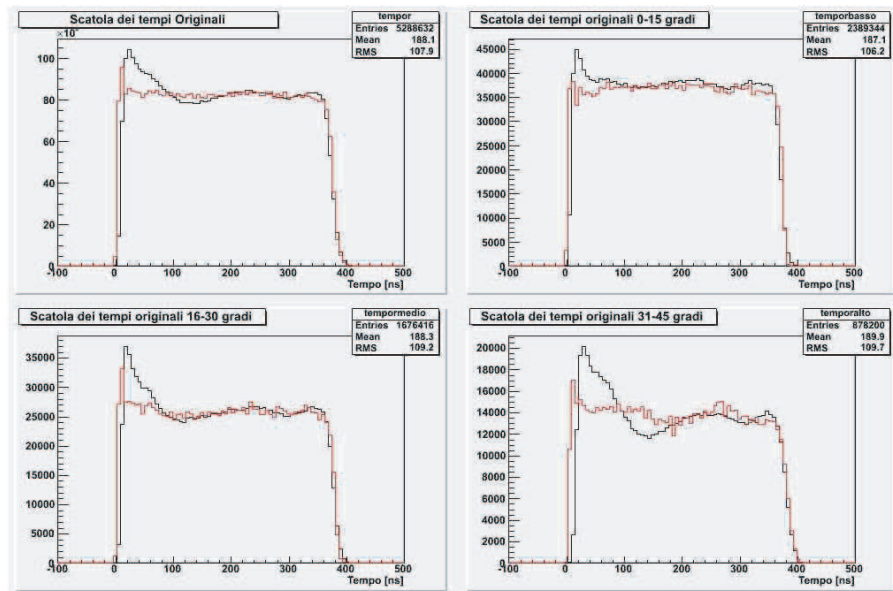


Figure 13: Time box histograms, before and after the drift time correction, for different track angle intervals.

plane, but are important for large angle tracks. At 45 degrees the effect of non linearity is shown to be about  $250\mu$  on average. The same method could be used to measure the space-time relation for the chambers in CMS, particularly in the regions where the presence of magnetic field is known to change sizeably the drift time-space dependence.

## References

- [1] “The CMS muon project, CMS Technical Design Report”, CERN/LHCC 97-32, CMS TDR, december 1997.
- [2] M. Benettoni, G. Bonomi, F. Gasparini, F. Gonella, A. Meneguzzo, S. Vanini, G. Zumerle, “CMS DT Chambers: Optimized Measurement of Cosmic Rays Crossing Time in absence of Magnetic Field”, CMS Note 2007/000.
- [3] M. Aguilar-Benitez et al., “Construction and test of the final CMS Barrel Drift Tube Muon Chamber prototype”, Nucl. Instrum. Meth. A **480** (2002) 658
- [4] J. Puerta Pelayo, M.C. Fouz, P. Garcia-Abia, “Parametrization of the Response of the Muon Barrel Drift Tubes”, CMS Note 2005/018.
- [5] R. Veenhof, “GARFIELD. Simulation of gaseous detectors”, CERN Writeups, Ref. W5050.
- [6] M. Cavicchi, F. Gonella, I. Lippi, P. Guaita, M. Pegoraro, E. Torassa, “Properties and Performances of a Front-end ASIC Prototype for the Readout of the CMS Barrel Muon Drift Tubes Chambers”, CMS Note 1999/033.
- [7] CMS Collaboration, “Level-1 Trigger Technical Design Report”, CERN LHCC 2000-038.
- [8] C. Fernandez Bedoya, J. Marin, J. C. Oller and C. Willmott, “Electronics For The Cms Muon Drift Tube Chambers: The Read-Out Minicrate”, IEEE Trans. Nucl. Sci. **52** (2005) 944
- [9] M. Benettoni et al., “Performance of the drift tubes for the barrel muon chambers of the CMS detector at LHC”, Nucl. Instrum. Meth. A **410** (1998) 133.
- [10] The Object Reconstruction for CMS Analysis program (ORCA), <http://cmsdoc.cern.ch/orca/>.
- [11] F.R. Cavallo et al., “Test of CMS Muon Barrel Drift Chambers with Cosmic Rays”, CMS Note 2003/017.
- [12] M. Benettoni et al., “Study of the Internal Alignment of the CMS Muon Barrel Drift Chambers using Cosmic Rays Tracks”, CMS Note 2004/001.
- [13] C. Albajar et al., “Test beam analysis of the first CMS drift tube muon chamber”, Nucl. Instrum. Meth. A **525** (2004) 465-484.